Biosensors and Bioelectronics 211 (2022) 114377

Contents lists available at ScienceDirect

Biosensors and Bioelectronics

journal homepage: www.elsevier.com/locate/bios

DropCRISPR: A LAMP-Cas12a based digital method for ultrasensitive detection of nucleic acid

Hui Wu [a,b,1], Xiaobao Cao [c,1], Yingchao Meng [b], Daniel Richards [b], Jian Wu [a,**], Zhangying Ye [a,*], Andrew J. deMello [b,***]

[a] College of Biosystems Engineering and Food Science, Zhejiang University, Hangzhou, 310058, China
[b] Department of Chemistry and Applied Biosciences, ETH Zurich, Vladimir Prelog Weg 1, Zurich, 8093, Switzerland
[c] Guangzhou Laboratory, International Bio Island, Haizhu District, Guangzhou, Guangdong, China

ARTICLE INFO

Keywords:
Droplet microfluidics
Salmonella typhimurium
Nucleic acid
Loop-mediated isothermal amplification
CRISPR/Cas12a

ABSTRACT

Since their discovery, CRISPR/Cas systems have been extensively exploited in nucleic acid biosensing. However, the vast majority of contemporary platforms offer only qualitative detection of nucleic acid, and fail to realize ultrasensitive quantitative detection. Herein, we report a digital droplet-based platform (DropCRISPR), which combines loop-mediated isothermal amplification (LAMP) with CRISPR/Cas12a to realize ultrasensitive and quantitative detection of nucleic acids. This is achieved through a novel two-step microfluidic system which combines droplet LAMP with a picoinjector capable of injecting the required CRISPR/Cas12a reagents into each droplet. This method circumvents the temperature incompatibilities of LAMP and CRISPR/Cas12a and avoids mutual interference between amplification reaction and CRISPR detection. Ultrasensitive detection (at fM level) was achieved for a model plasmid containing the *invA* gene of *Salmonella typhimurium* (*St*), with detection down to 10^2 cfu/mL being achieved in pure bacterial culture. Additionally, we demonstrate that the DropCRISPR platform is capable of detecting *St* in raw milk samples without additional nucleic acid extraction. The sensitivity and robustness of the DropCRISPR further demonstrates the potential of CRISPR/Cas-based diagnostic platforms, particularly when combined with state-of-the-art microfluidic architectures.

1. Introduction

In vitro diagnostics (IVDs) have revolutionized how medical professionals approach disease identification and treatment. This revolution has been led in part by nucleic acid detection, which allows the differentiation of diseases at the molecular level. Nucleic acid testing is routinely employed in range of fields, including medical diagnosis, food safety monitoring and the detection of environmental toxins (Hellou et al., 2021; Mangal et al., 2016). The importance and ubiquity of testing for nucleic acid targets has been perfectly exemplified by the SARS-CoV-2 outbreak, with nucleic acid amplification tests (NAATs) being the gold-standard for ultra-sensitive detection and variant differentiation (Esbin et al., 2020; Zhang et al., 2020). Given their excellent sensitivity and specificity (Deng and Gao, 2015; Kang, 2019; Wu et al., 2020b), the reliance on NAAT-based methods is unsurprising. Whilst many methods exist for nucleic acid amplification, polymerase chain reaction (PCR) is still generally regarded as the go-to tool for nucleic acid analysis. However, PCR typically requires the use of high-cost thermocyclers and long reaction times, which limits the utility technique. Several isothermal amplification methods, such as loop-mediated isothermal amplification (LAMP) and recombinase polymerase amplification (RPA), have been developed as alternatives to PCR due to their convenience, rapidity and low cost (Li et al., 2017; Lobato and O'Sullivan, 2018; Zhao et al., 2015).

Digital nucleic acid amplification detection is a sensitive and accurate method for the absolute quantification of nucleic acids (Huggett et al., 2015; Quan et al., 2018), and operates by distributing a target into a large number of independent partitions, with each partition containing no more than one target molecule. After amplification, target concentrations can be calculated by the simple detection of signal and analysis

* Corresponding author.
** Corresponding author.
*** Corresponding author.
E-mail addresses: wujian69@zju.edu.cn (J. Wu), yzyzju@zju.edu.cn (Z. Ye), andrew.demello@chem.ethz.ch (A.J. deMello).
[1] These authors contribute equally to the article.

https://doi.org/10.1016/j.bios.2022.114377
Received 2 March 2022; Received in revised form 12 May 2022; Accepted 13 May 2022
Available online 18 May 2022

of Poisson statistics based on the ratio of positive and negative partitions. Such techniques preclude the need to build a standard curve and are typically more precise, robust, and reproducible than conventional methods (Hindson et al., 2013). In this regard, digital detection methods are particularly attractive for pathogen detection and medical diagnoses, where accurate quantification of disease load is important for informing treatment pathways (Yu et al., 2020). Over the last 15 years, several microchamber array and droplet-based digital detection platforms have been reported (Bhat et al., 2009; Li et al., 2016; Rane et al., 2015). However, for digital nucleic acid detection, several limiting problems are still unaddressed. For example, the signal difference between positive and negative reaction partitions (signal:noise) can often be low, necessitating the use of complex optical setups for differentiation (Chen et al., 2017). Additionally, non-specific amplification can seriously affect the accuracy of detection results by returning false-positive partitions (Rolando et al., 2020). Accordingly, methods for boosting signals and improving specificity are highly sought after.

Recently, CRISPR/Cas based nucleic acid detection methods for improving both sensitivity and specificity have been reported. Based on the cis cleavage activity of Cas9, some researchers used gene circuits coupled with Cas9 to achieve qualitative nucleic acid analysis (Dai et al., 2020). Meantime, several other Cas proteins, such as Cas12a, Cas13a and Cas12b, activated by a guide RNA (gRNA)-target nucleic acid duplex, can unleash strong trans cleavage activity to cut non-specific single-stranded nucleic acids. This can be combined with quenched fluorescence probes to generate a strong signal. Through strategic coupling with NAAT, such Cas proteins have been used to develop the DETECTR (Chen et al., 2018), SHERLOCK (Gootenberg et al., 2017) and HOLMESv2 (Li et al., 2019a) platforms, which display high sensitivity and specificity for nucleic acid detection. The success of these platforms has led to NAAT-CRISPR/Cas systems being positioned as the next generation of molecular detection techniques (Li et al., 2019b; Wu et al., 2021a). However, such methods are almost always used for qualitative detection. To achieve quantitative detection, some groups have established digital CRISPR-based methods by combining RPA with CRISPR/Cas systems in commercial microarray chips (Park et al., 2021; Wu et al., 2021c). Whilst the low operating temperature of RPA can bring several advantages, it can also lead to higher background signals due to spontaneous reaction before digital reaction partitioning. These methods are also limited by their reliance on commercial devices, which typically contain $\leq$20,000 partitions and thus have a limited dynamic range. LAMP, a widely used isothermal amplification technique which operates at around 65 °C, typically displays a higher degree of specificity compared to RPA due to the larger number of target-specific primers (Notomi et al., 2000). LAMP has also been demonstrated in complex sample matrices, and has shown a remarkable resistance to reaction inhibition by contaminants (Francois et al., 2011). We previously described the benefits to sensitivity and specificity that can be gained by coupling LAMP with CRISPR/Cas12a (Qian et al., 2019; Wu et al., 2020a). However, to date, no digital nucleic acid assay based on LAMP and CRISPR/Cas12a has been reported.

Herein, we describe a droplet-digital LAMP-CRISPR/Cas12a assay platform (DropCRISPR) to achieve absolute quantitative analysis of nucleic acids. We demonstrate the platform using a nucleic acid target derived from *Salmonella typhimurium* (*St*), a common foodborne pathogen causing diarrhea, fever, and abdominal cramps in humans. We report a novel microfluidic architecture which combines droplet-digital LAMP with a picoinjector capable of introducing the CRISPR/Cas12a reagents directly into the droplets. The added signal amplification provided by this hybrid approach enables ultrasensitive detection of target nucleic acid, and the added specificity increases the accuracy of detection results and facilitates detection within unprocessed samples.

2. Materials and methods

2.1. Materials

The *St* strain was kindly provided by the institute for microbiology (Hardt Lab), ETH Zurich (Zurich, Switzerland). Primers, gRNAs and single-stranded DNA-FQ probes were synthesized by Microsynth (Balgach, Switzerland). The plasmid containing the *invA* gene of *St* was purchased from Thermo Fisher Scientific Inc. (Waltham, USA). The sequence information for all primers, gRNAs and probes can be found in Table S1. Nucleic acid extraction was performed using the GenElute Bacterial Genomic DNA Kit (Sigma-Aldrich Co. LLC., St. Louis, USA). Milk-1 (Milbona, lactose-free semi-skilled milk, UHT, item #5107921) and Milk-2 (Milbona, 0.1% skimmed milk, UHT, item #5106480) were purchased from Lidl Schweiz (Zürich, Switzerland).

2.2. LAMP reaction

Six primers (Table S1) were designed to specifically target eight regions of the *St*-specific *invA* gene. The length of the amplified fragment was 227 bp.

Bulk LAMP reaction: A LAMP MasterMix containing 0.2 μM F3-St, 0.2 μM B3-St, 1.6 μM FIP-St, 1.6 μM BIP-St, 0.4 μM LF-St, 0.4 μM LB-St, 0.8 M betaine (Sigma-Aldrich Co. LLC., St. Louis, USA), 0.35 mM dNTP each (Thermo Fisher Scientific Inc., Waltham, USA), 1 × ThermoPol buffer, 2 mM $MgSO_4$, and 0.64 U/μL *Bst* DNA polymerase, Large Fragment (New England Biolabs Inc., Ipswich, USA) was prepared. To 21.25 μL of this MasterMix, 2.5 μL of the target was added at the desired concentration, followed by 1.25 μL of 20 × EvaGreen (Biotium, Inc, Fremont, USA), and the reaction incubated at 63 °C for 60 min. The reaction was followed on a QuantStudio 3 Real-time PCR system (Thermo Fisher Scientific Inc., Waltham, USA). The threshold time (T_t) was calculated by the software and reported without further manipulation.

Digital droplet LAMP reaction: To 9 μL of the LAMP MasterMix (see *Bulk LAMP reaction*), 1 μL of the target was added. For direct analysis of the LAMP products (Fig. 1), EvaGreen was added to the MasterMix at a total concentration of 1 × . This mixture was immediately injected into the droplet generator to act as the dispersed phase. Hydrofluoroether (HFE) 7500 oil (3 M, St. Paul, USA) containing 5% (w/w) 008-FluoroSurfactant (RAN Biotechnologies, Beverly, USA) was used as the continuous phase. The oil and reaction solutions were respectively injected into the two inlets of chip using an air pressure pump (OB1 MK2, Elvesys, Paris, France) to produce water-in-oil droplets with a diameter of ~30 μm and at a frequency of 1.3 kHz. Total consumption of the initial volume was achieved within 10 min. The generated droplets were collected into PCR tube and then incubated at 63 °C for 50 min.

2.3. Digital CRISPR/Cas12a detection

For optimized CRISPR/Cas12a detection, a MasterMix containing 1 × NEBuffer 2.1, 200 nM Cas12a protein (New England Biolabs Inc., Ipswich, USA), 600 nM gRNA, 2.5 μM single-stranded DNA-FQ probe (Microsynth, Balgach, Switzerland) and 0.5 U/μL RNase inhibitor (Thermo Fisher Scientific Inc., Waltham, USA) was prepared and connected to the picoinjector orifice via an inlet. The droplets from the LAMP reaction were introduced into the picoinjector chip via another inlet, and Hydrofluoroether (HFE) 7500 oil containing 5% (w/w) 008-FluoroSurfactant was added via a side channel to increase droplet spacing. Picoinjection of the CRISPR/Cas12a MasterMix into the LAMP droplets was achieved using electrodes energized by an amplifier (TREK 623B, Advanced Energy Industries, Inc., Fort Collins, USA), and a function generator (33210A, Agilent Technologies, Inc., Santa Clara, USA) outputting a 1 kHz sinusoidal signal ranging from 0 to 150 mV. The droplets were collected in a PCR tube and then heated at 42 °C to facilitate trans cleavage of the fluorescent reporter probe.

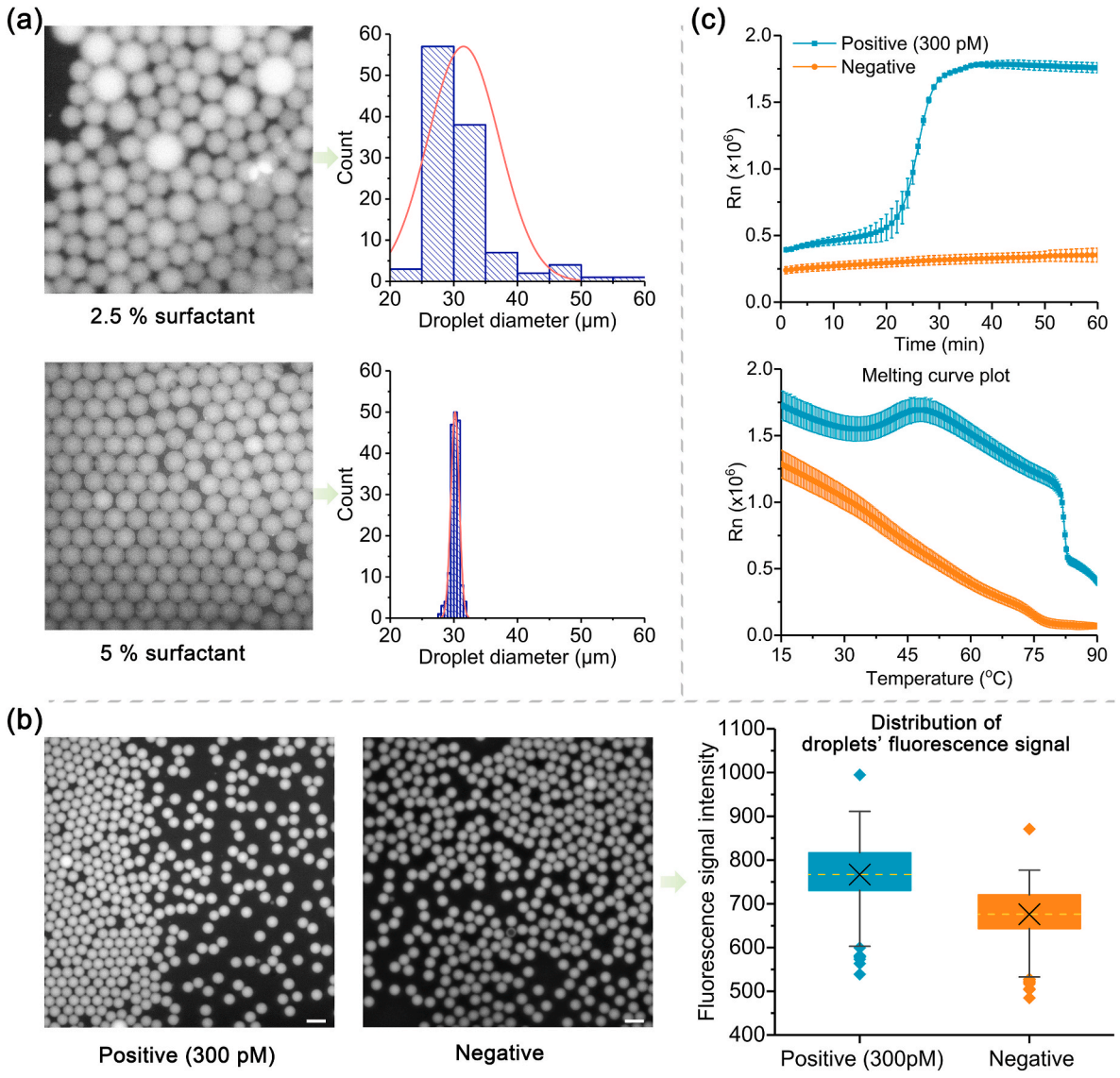

Fig. 1. (a) Brightfield images and histograms of droplets generated using an HFE7500 carrier fluid containing 2.5% and 5% of 008-FluoroSurfactant. Droplets were incubated at 63 °C for 50 min prior to imaging; (b) Fluorescence images of droplets containing LAMP reagents and EvaGreen. Positive droplets were generated from buffer containing 300 pM of the target *invA* DNA. Negative control contained no target. The scale bar is 50 μm. No statistical difference was observed between the two populations (n = 423); (c) Amplification and melting-curve analysis of a bulk LAMP reaction containing 300 pM of *invA* DNA. The negative control contains only sterile H_2O. The results are plotted as a mean ± SD (N = 3).

2.4. The fabrication of droplet generator and picoinjector

The cross-junction microfluidic droplet generator was fabricated in PDMS according to standard soft lithographic procedures (Zhao et al., 1997). Microfluidic channel patterns (Fig. S1) were designed using AutoCAD and printed onto high-resolution photolithographic masks (Micro Lithography Services Ltd., Chelmsford, U.K.). An SU-8 master mold, which had a layer height of 40 μm, was fabricated via standard photolithography. Subsequently, the SU-8 mold was exposed to a chlorotrimethylsilane (Sigma-Aldrich Co. LLC., St. Louis, USA) vapor for at least 30 min at room temperature to facilitate the subsequent separation of PDMS from the mold. A 10:1 (w/w) mixture of PDMS base to curing agent (Sylgard 184, Dow Corning, Midland, USA) was poured onto the master mold, degassed for 30 min and cured at 70 °C for 60 min. Then, the PDMS was peeled from the mold and diced. A hole puncher (Syneo, Florida, USA) was used to create two inlets and one outlet at the desired positions. Afterwards, the structured PDMS substrate was bonded to a thin layer of PDMS-covered glass slide after a 60 s exposure in an oxygen plasma (EMITECH K1000X, Quorum Technologies, East Sussex, UK). The constructed droplet generator was finally left on a hot plate at 120 °C overnight.

A picoinjector was used to inject reagents into droplets (Abate et al., 2010). The two-dimensional channel pattern of the picoinjector is provided in Fig. S2. In this study, a two-photon polymerization (TPP) technology using the Photonic Professional GT system (Nanoscribe GmbH, Eggenstein-Leopoldshafen, Germany), equipped with a 25 × NA 0.8 plan apochromat air objective lens (Zeiss, Oberkochen, Germany), was used to 3D print the picoinjector mold. An aliquot of IP-S photoresist (Nanoscribe GmbH, Eggenstein-Leopoldshafen, Germany) was dropped onto an indium tin oxide (ITO)-coated glass substrate. During printing, the IP-S photoresist was exposed to a 780 nm fs laser and features printed in a layer-by-layer fashion. The slicing and hatching distances were set to 1.0 and 0.5 μm, respectively. After printing, the mold was first developed in 1-methoxy-2-propanol acetate (Sigma-Aldrich, Buchs, Switzerland) for 20 min, then washed in isopropanol for 5 min and finally baked in an oven at 200 °C for 2 h. Next, a 10:1 (w/w) mixture of

PDMS base to curing agent (Sylgard 184, Dow Corning, Midland, USA) was used to fabricate the PDMS replica that was bonded to a thin layer of PDMS-covered glass slide after a 60 s exposure to an oxygen plasma. The constructed picoinjector was then left on a hot plate at 120 °C overnight.

2.5. Droplet imaging

To allow efficient imaging of droplets, a HybriWell Sealing System (SKU# 612107, Grace Bio Labs, Bend, USA) was adhered to a 1 mm thick glass slide, forming a sealed chamber ($9.8 \times 20 \times 0.25$ mm^3) containing two 1.5 mm diameter ports. Processed droplets were pipetted into the chamber, and the ports covered with sealing tabs (SKU# 629200, Grace Bio Labs, Bend, USA) to prevent evaporation. The chamber was placed on an inverted microscope (Nikon Ti-E Microscope, Zurich, Switzerland) containing a motorized x-y translation stage. For fluorescence signal measurements, a high-power cyan (488 nm) LED light source (SPECTRA X light engine, Lumencor, Beaverton, USA) was used as an excitation source. The beam was reflected by a dichroic mirror (ZT 488/Chroma AHF, Tübingen, Germany) and focused into the chamber through a Plan Fluor 20 × NA 0.45 objective (Nikon, Zurich, Switzerland). Emitted light was passed through a filter (520/25 nm, Chroma AHF, Tübingen, Germany), collected by the objective, and detected by a digital CMOS camera (ORCA-Flash4.0, C11440, Hamamatsu Photonics K.K., Hamamatsu, Japan). Brightfield images were captured using the same CMOS camera without the use of optical filters.

3. Results and discussion

3.1. Droplet digital LAMP

To facilitate the digital LAMP assay, we first developed a microfluidic device capable of partitioning the LAMP reagents into stable droplets (Fig. S1). We assessed this chip using LAMP reaction mixtures containing the necessary reagents, primers and the intercalating dye EvaGreen as the dispersed phase. The continuous phase consisted of HFE 7500 oil containing 008-FluoroSurfactant at various concentrations. To assess stability, the droplets were collected in PCR tubes and heated at 63 °C for 50 min. We observed that droplet stability was controlled by the concentration of the 008-FluoroSurfactant, with droplet merging occurring at lower surfactant concentrations. However, at 5% (w/w) surfactant concentrations the droplets were fully stable over the entire period of observation, and remained monodisperse with an average diameter of ~30 μm (Fig. 1a).

Subsequently, we used the droplet digital LAMP to perform quantitative detection of a plasmid containing the *invA* gene of *St*. Droplets containing all the necessary reagents were incubated at 63 °C for 50 min, collected, and then imaged using an inverted fluorescence microscope. No significant difference in fluorescence signal was observed between the sample and the negative (no target) control (Fig. 1b). As a positive control, we performed the LAMP reaction in bulk and observed the expected amplification curve (Fig. 1c). Melting curve analysis highlighted the high fluorescence background of the negative LAMP mixtures at room temperature as a potential cause of the high background observed in the droplets (Fig. 1c). To confirm that this result was generalizable to different intercalating dyes, we replicated the melt curve analysis with SYBR Green and observed a similar result (Fig. S3). We hypothesize that this phenomenon results from homo- and hetero-primer dimers formed by the large number (six) and concentration of primers required for LAMP. This explains why the background fluorescence decreases as the temperature increases (the primers dissociate), and why the problem is exacerbated in droplets (a higher local concentration). These results demonstrate that the combination of LAMP and intercalating dyes is unsuitable for the digital detection of the nucleic acid target. Whilst there have been some reported of droplet or microchamber array based-digital LAMP methods using intercalating dyes and having low fluorescence background, associated sensitivities are typically lower (Nixon et al., 2014; Rolando et al., 2019; Sun et al., 2013; Yuan et al., 2021). It should be noted that calcein-based dye for use in digital LAMP have been reported, although these are not suitable for ultra-sensitive detection (Lin et al., 2019; Rane et al., 2015; Zhu et al., 2012). Also, fluorescence probe can be used for digital LAMP, but the design of probe is relatively complicated (Schuler et al., 2016). Clearly, methods for further amplifying the signal with simple strategies are required for ultra-sensitive detection.

3.2. Construction of DropCRISPR by picoinjector

In our previous work, we showed that coupling LAMP with CRISPR/Cas12a led to significant signal amplification and enabled highly specific and sensitive target detection in bulk assays (Qian et al., 2019; Wu et al., 2020a). Thus, we hypothesized that this system could operate in droplets, creating a powerful digital platform for reliable and ultra-sensitive target quantification. To realize this, we first developed a system for introducing the necessary CRISPR/Cas12a reagents into the LAMP droplets. Due to the different optimal reaction temperatures of the *Bst* polymerase and Cas12a, encapsulating both the LAMP and CRISPR/Cas reagents in droplets at the same time led to unsatisfactory results (data not shown). Instead, we designed a microfluidic device containing a picoinjector to actively introduce the CRISPR/Cas12a reagents into the droplets after the LAMP reaction (Fig. 2a). The architecture of the device forces the droplets into single file before they pass the picoinjector, which introduces the necessary reagents. The picoinjector is comprised of a pressurized channel containing the reagents to be added and a positive and negative electrode. When the droplets flow past the picoinjector, the electric field destabilizes the water-oil interface, allowing the reagents to enter the droplet. Once the droplets leave the vicinity of the electric field, they regain their stability. To simplify the fabrication of the electrodes, two empty PDMS channels were placed in the proximity of the picoinjector orifice and filled with a saturated sodium chloride solution. The two electrodes of the amplifier were subsequently connected to the two PDMS channels using metal needles. We designed two picoinjection structures of differing reagent orifice length (10 μm and 1 μm). The performance of the two picoinjector architectures was assessed by injecting black ink into droplets produced by the digital LAMP droplet generator (Fig. 2b, Video S1/S2). The channel containing the black ink was maintained at a high pressure to facilitate fluid injection into the droplets. A high curvature interface between the black ink and the oil was observed due to the small orifice, which maintained the balance of the forces on the interface. When employing the 10 μm picoinjector orifice, a lower ink injection efficiency was observed. We also observed pressure fluctuations in the oil channel during droplet flow. When the length of the orifice was shortened to 1 μm, these problems disappeared, and perfect injection of the ink into every droplet could be achieved (Video S2). We hypothesize that the longer orifice causes a greater disturbance to the balance of injection process, and thus resulting in some droplets not being injected into the ink.

Supplementary data related to this article can be found at https://doi.org/10.1016/j.bios.2022.114377.

Once optimized, the picoinjection structure with a 1 μm orifice length was combined with the droplet generator to construct the DropCRISPR platform (Fig. 2c). The droplets containing the LAMP reagents (without dye) and the target were first produced using the previously optimized droplet generator (Fig. 1), collected, and then incubated at 63 °C for 50 min. The droplets were subsequently introduced into the picoinjection chip, which was pre-filled with the CRISPR/Cas12a reagents (Cas12a proteins, gRNAs, fluorescent probes), using an air pressure pump. By optimizing the electric field and the pressures of the oil (~90 mBar), droplet injection (~160 mBar), and picoinjection channels (~85 mBar), each flowing droplet could be accurately injected with the necessary reagents (Video S3). Processing of the entire LAMP mixture (10 μL) to produce approximately 7×10^5 droplets could be

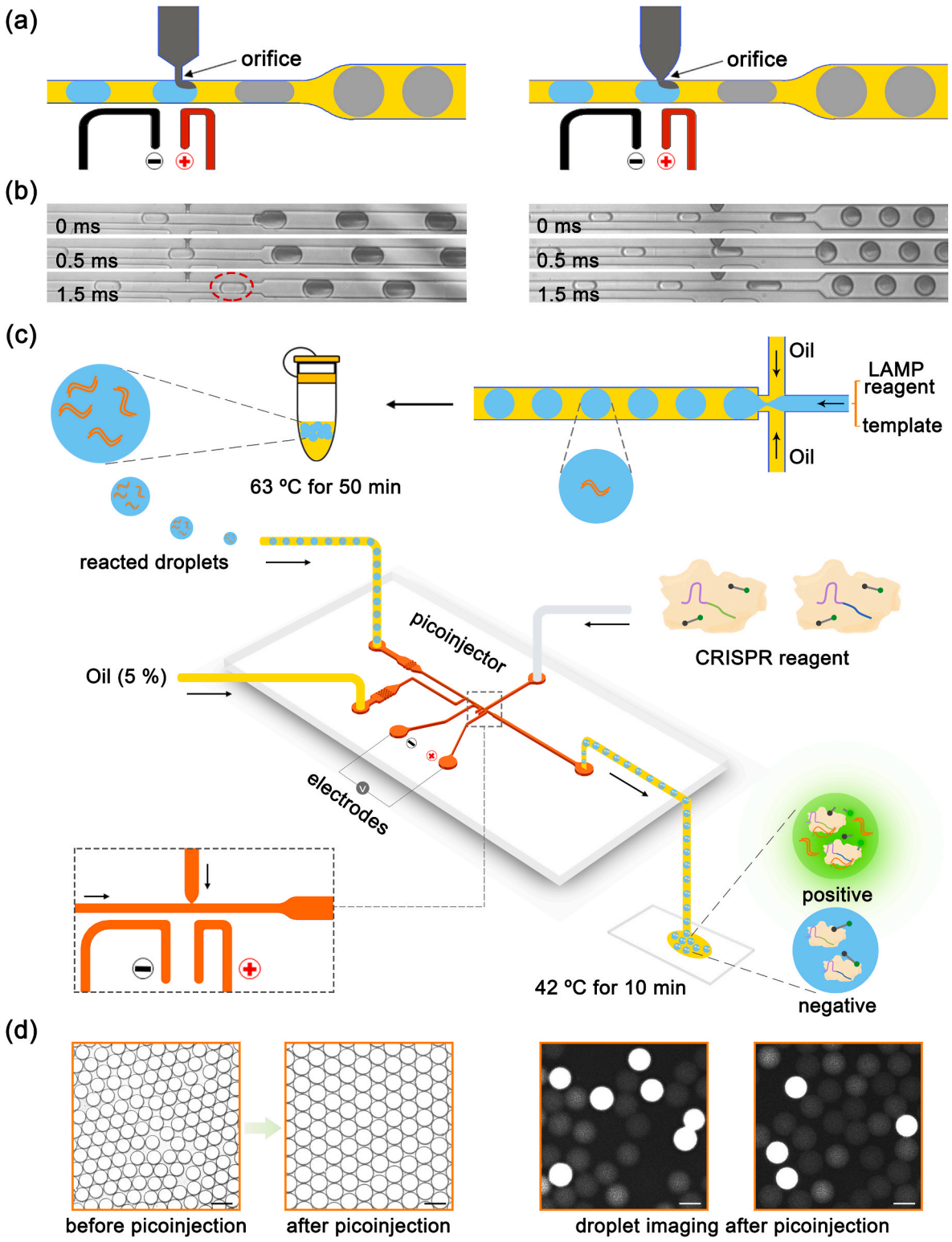

Fig. 2. (a) Schematic representations of two picoinjection structures with 10 μm (left) and 1 μm (right) orifice lengths; (b) Time course brightfield images of droplets injected with black ink via the picoinjector; (c) A schematic diagram of the hybrid LAMP-CRISPR/Cas12a DropCRISPR platform; (d) Brightfield images showing the change of droplet diameter before and after picoinjection, and representative fluorescence images obtained after CRISPR/Cas12a mediated signal generation. The scale bar is 50 μm.

completed within 20 min. After picoinjection, the diameter of droplets increased from ~30 μm to 40 μm (Fig. 2d), which is consistent with a volume increase of ~19 pL. The droplets produced by the chip were then collected, incubated at 42 °C for 10 min and imaged using an inverted fluorescence microscope (Fig. 2d).

Supplementary data related to this article can be found at https://doi.org/10.1016/j.bios.2022.114377.

Initial results provide clear demonstration of the potential of Drop-CRISPR. Significant signal observed in the droplets containing template proved the CRISPR/Cas12a process was taking place. Inside each droplet

containing the target, the amplicons are captured by the binary complex of Cas12a/gRNA, activating the trans cleavage activity of Cas12a to cut the single-stranded DNA-FQ probe and produce a fluorescence signal. Since the trans cleavage activity of the Cas12a protein is catalytic, this process leads to signal amplification and significant sensitivity enhancement. With 3 pM of plasmid containing the *invA* gene target, positive droplets produced a measurable fluorescence signal whilst almost no fluorescence was observed in droplets containing no target (Fig. 2d). This is in stark contrast to the droplet digital LAMP reaction without addition of CRISPR/Cas12a, where the background of the negative droplets was high (Fig. 1b). These results clearly demonstrate the benefits of combining LAMP with CRISPR/Cas12a in droplets.

3.3. Optimization of CRISPR/Cas12a detection system

For digital nucleic acid detection, the primary factor determining sensitivity and time-to-result is the signal-to-noise ratio. To maximize this important parameter, we decided to optimize the signal amplification capacity of the CRISPR/Cas12a reaction. The concentration of each CRISPR/Cas12a component for LAMP amplicon detection has been previously optimized (Wu et al., 2020a). Thus, in this work we optimized the gRNA structure and reaction temperature. We designed two gRNA sequences, one which was complementary to the central region of the target (gRNA-1), and a second which was complementary at the 3′end (gRNA-2) (Fig. 3a). We then assessed the ability of these gRNAs to initiate catalytic cleavage by monitoring the signal generated from cleavage of the DNA-FQ probe in the presence of 3 nM of the *invA* target

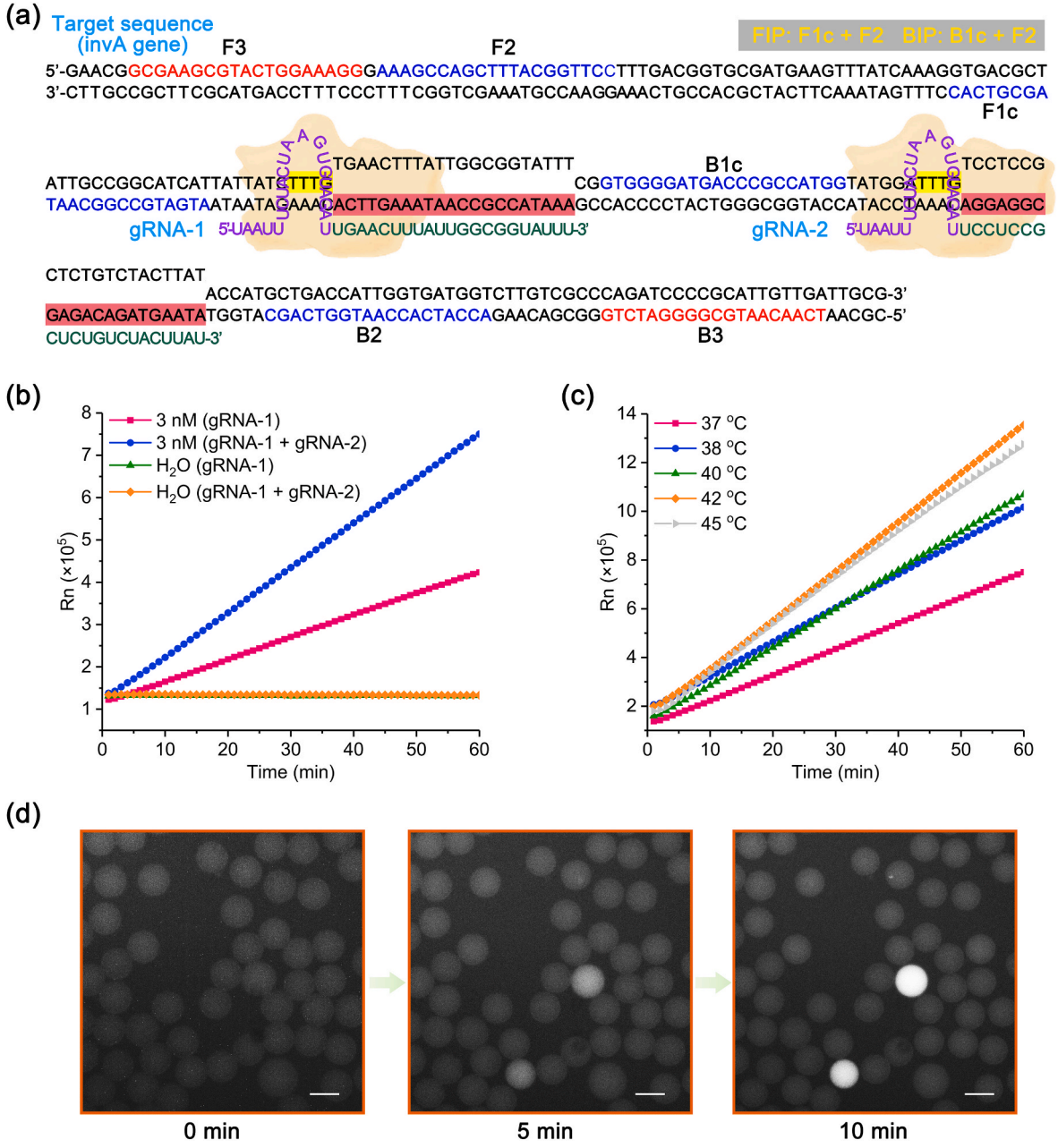

Fig. 3. (a) Sequence information for the LAMP amplicon (*invA* gene) and the two designed gRNAs (gRNA-1, gRNA-2); (b) CRISPR/Cas12a detection of plasmid containing the *invA* gene target using either one or two gRNAs; (c) CRISPR/Cas12a detection of plasmid containing the *invA* gene target at different temperatures. The concentration of plasmid was 3 nM for both experiments; (d) Time course fluorescence microscope images of CRISPR/Cas12a amplification in droplets. The initial target concentration for LAMP amplification was 300 fM. The scale bar is 40 μm.

at 37 °C (Fig. 3b). The data show that significant improvements in signal generation can be achieved when both gRNA-1 and gRNA-2 are employed together. This can likely be attributed to each target now recruiting two Cas12a proteins rather than one. This would lead to a significant increase in trans cleavage activity. Based on these data, we added both gRNAs to the reactions in all subsequent experiments. Next, again employing 3 nM of the *invA* target, we explored the effect of temperature on the CRISPR/Cas12a detection system (Fig. 3c). The data show a clear advantage to performing the CRISPR/Cas12a reaction at 42 °C.

Once both the LAMP and CRISPR/Cas12a reactions were optimized, we transferred them into the combined DropCRISPR platform. Droplets ~14 pL in volume (~30 μm) were produced containing the LAMP reagents and 300 fM of the *invA* target, and heated at 63 °C for 50 min. Droplets were subsequently passed through the picoinjector chip, and 19 pL of the CRISPR/Cas12a reaction mixture was injected into each droplet. According to our previous research (Wu et al. 2020a, 2021b), a 1:1 ratio of LAMP to CRISPR/Cas12a reagents works well; thus, the volume ratio achieved here was suitable. The droplets were heated at 42 °C on a hotplate and samples were taken at 0, 5, and 10 min to be imaged under a fluorescence microscope (Fig. 3d). Under these conditions the reaction proceeded rapidly with fluorescence signal being observed at 5 min, though the signal-to-noise ratio was noticeably improved at 10 min. When combined, the data demonstrate that under the optimized conditions the CRISPR/Cas12a reaction proceeds efficiently in droplets.

3.4. Performance of DropCRISPR for plasmid and St strain detection

To evaluate the analytical performance of the DropCRISPR platform, we first tested the system using a buffered dilution series of a plasmid containing the *invA* gene (Fig. 4c and d). We compared this to a LAMP reaction in bulk (Fig. 4a), and a LAMP/Cas12a reaction in bulk (Fig. 4b). For the DropCRISPR platform, we observed a limit of detection as low as 3 fM, two orders of magnitude lower than both the bulk LAMP reaction and bulk LAMP/Cas12a reaction (~300 fM). The number of positive droplets decreased proportionally as the target DNA concentration decreased (Fig. 4c). To verify the reproducibility of this method, three independent DropCRISPR experiments on three different days were tested, across a broad range of target concentrations (3–3000 fM) (Fig. 4d). Linear regression was performed, and the correlation coefficient (R^2) value was >0.99 across the range of concentrations. Additionally, the standard deviations (SD) at each concentration were all <15%. Comparison of the theoretical positive droplet percentage vs

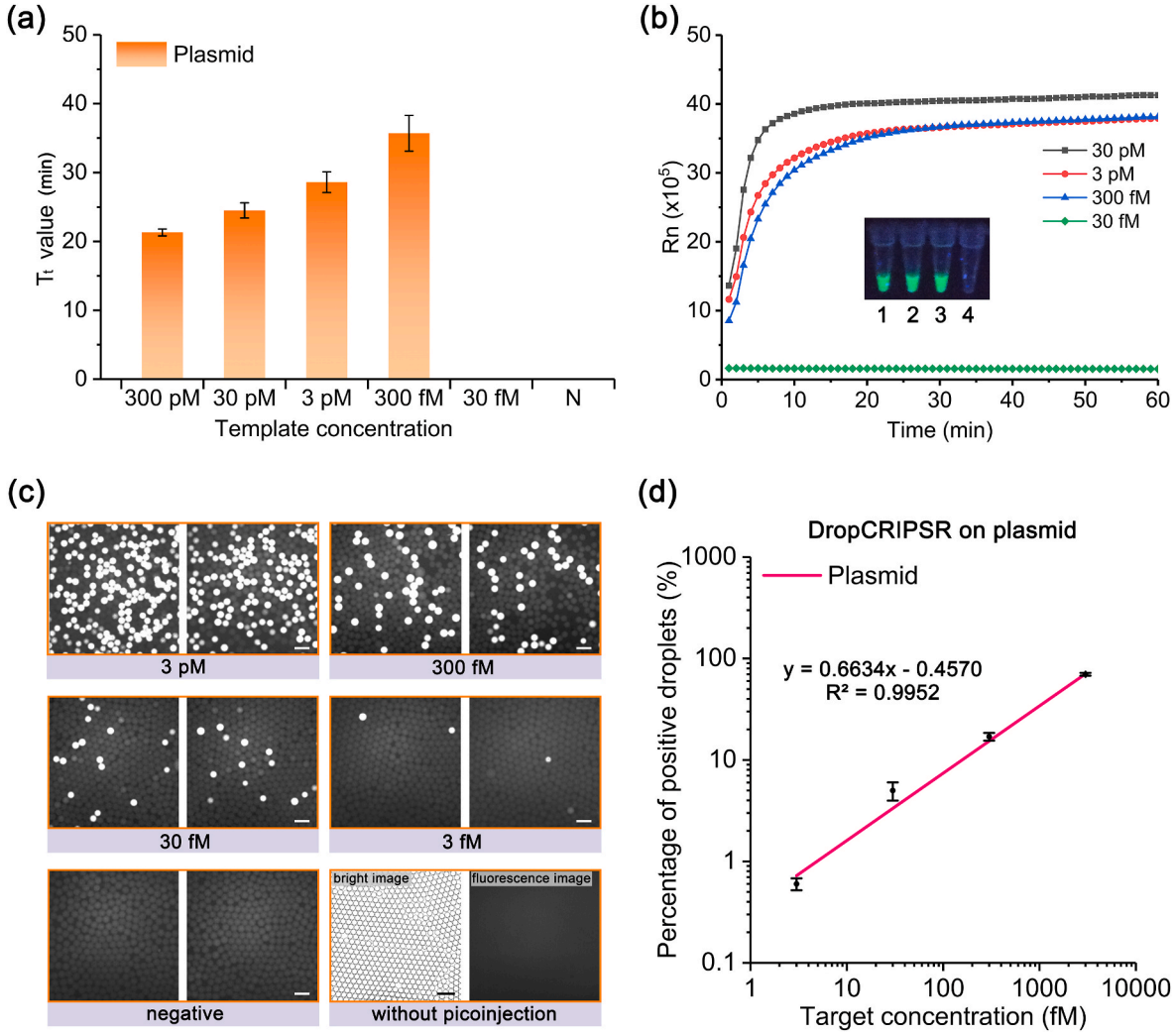

Fig. 4. (a) Bulk real-time LAMP detection of the *invA* gene of *St*. Threshold time (T_t) was determined and used as a measure of detection limit; (b) Evaluation of the detection sensitivity of bulk LAMP-CRISPR/Cas12a. The inset fluorescence image was obtained by using UV lamp (302 nm) to irradiate the reaction solution at room temperature after LAMP-CRISPR/Cas12a reaction. The numbers "1, 2, 3, 4" represent "30 pM, 3 pM, 300 fM, 30 fM", respectively; (c) Fluorescence images of droplets generated using the DropCRISPR platform from different input target concentrations. No signal is detected without picoinjection of the CRISPR/Cas12a reagents. The scale bar is 100 μm; (d) Percentage of positive droplets vs input target concentration. In each graph the results are plotted as a mean ± SD (N = 3).

experimental droplet percentage (Fig. S4) shows good agreement, proving that the DropCRISPR is capable of realizing ultrasensitive and quantitative detection. Taken together, these experiments confirm that DropCRISPR is capable of producing highly accurate and reproducible data. The high signal observed from DropCRISPR can be attributed to the catalytic trans cleavage capabilities of the Cas12a protein, as well as the confinement effect of the droplets (Fig. S5). By utilizing small droplet sizes (~30 μm diameter), even a single copy of DNA inside a droplet corresponds to a concentration of 120 fM. This is high enough to initiate LAMP reaction and significant trans cleavage of the DNA–FQ reporter by Cas12a.

Once optimized, we used the DropCRISPR platform to detect a cultured *St* bacterial strain. The *St* bacterial strain was cultivated overnight in LB (Luria-Bertani) liquid medium at 37 °C, and the concentration of the bulk solution was determined (10^7 cfu/mL) by checking the OD value at 600 nm. We subsequently prepared a serial dilution range of different concentrations of *St* (10^2–10^7 cfu/mL). The DNA was extracted and diluted into Tris-EDTA (TE) buffer, and subsequently analyzed using the DropCRISPR platform (Fig. 5b). A linear relationship was observed between the *St* concentration and number of positive droplets (R^2 =

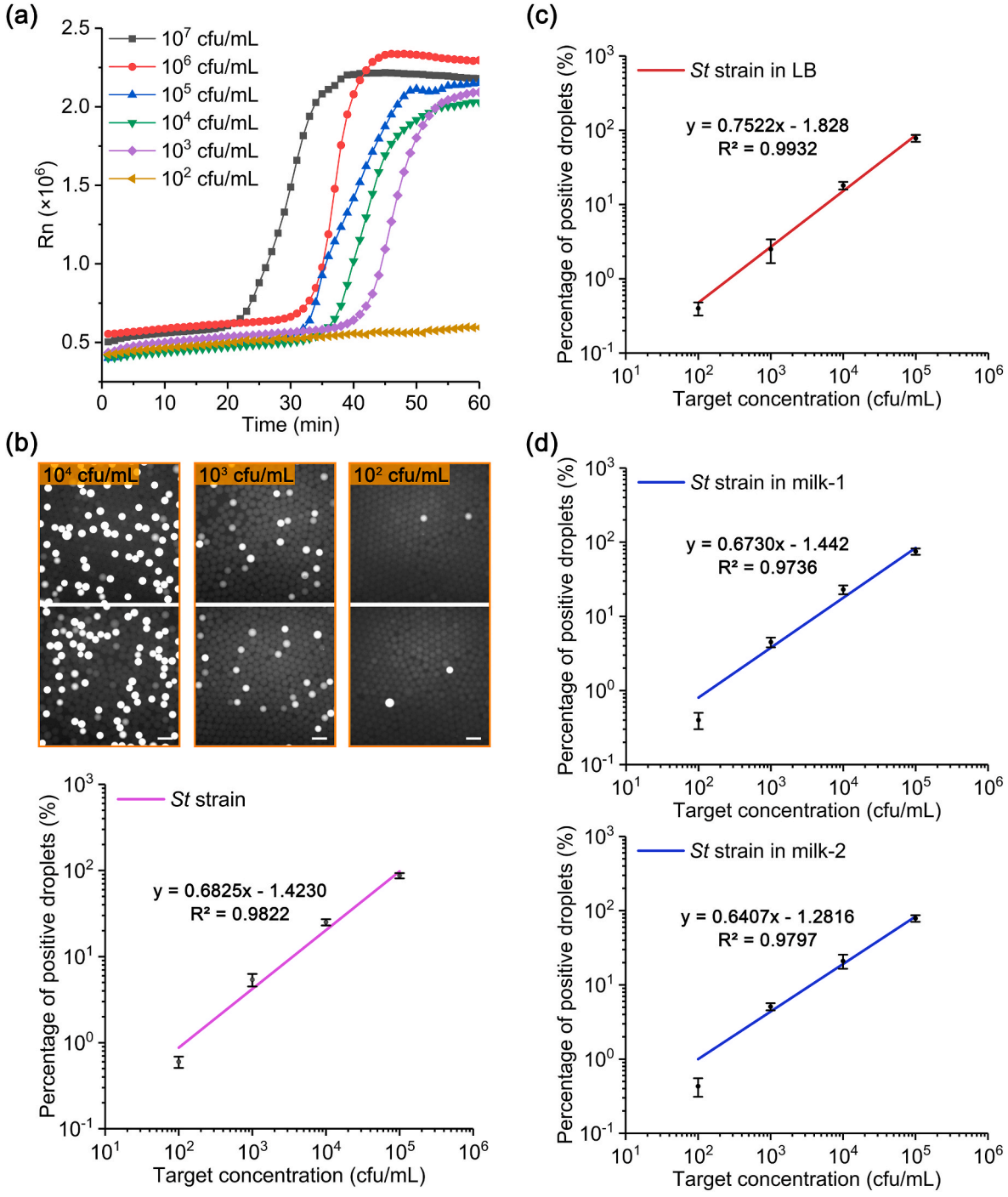

Fig. 5. (a) Bulk LAMP detection of the *invA* gene extracted from cultured *St*; (b) Representative fluorescence images of droplets generated from mixtures containing different concentrations of the *invA* gene extracted from cultured *St*. The plot shows the percentage of positive droplets vs input target concentration. The scale bar is 40 μm; (c) Percentage of positive droplets vs input target concentration for *St* cultured in LB. No DNA extraction or purification was performed; (d) Percentage of positive droplets vs input target concentration for cultured *St* spiked into two different types of milk. In each graph the results are plotted as a mean ± SD (N = 3).

0.9822), and the standard deviation (N = 3) between measurements at each concentration was <18%. A limit of detection of 10^2 cfu/mL was reached, which is an order of magnitude higher than the LAMP reaction in bulk (10^3 cfu/mL) (Fig. 5a). We also performed qPCR on the same samples, and observed a limit-of-detection comparable to bulk LAMP (Fig. S6). Put simply, the data demonstrate the capacity of DropCRISPR to significantly outperform bulk assays.

3.5. Direct St strain detection in raw samples by DropCRISPR

Due to the high sensitivity and specificity imparted by the hybrid LAMP-CRISPR/Cas12a approach, we hypothesized that the DropCRISPR platform could be used for direct *St* strain detection in raw samples and without sample preparation. We also theorized that the DNA extraction step could be omitted due to the high operating temperature of LAMP (63 °C), which should be sufficient to lyse the bacterial cells and release the DNA. To test this hypothesis, we compared bulk LAMP with and without a dedicated DNA extraction step across a range of *St* concentrations in LB medium (10^3–10^7 cfu/mL) (Fig. S7). We observed that without a dedicated DNA extraction step, the sensitivity of the assay decreased, with the limit of detection of 10^4 cfu/mL; an order of magnitude higher than that obtained using a dedicated bacteria extraction protocol (Fig. 5a). This indicates that bacteria lysis at 63 °C is not as efficient as a dedicated chemical bacteria lysis procedure. Additionally, the use of LB media resulted in substantial background signal in the bulk assays (Fig. S7). Notwithstanding, the DropCRISPR platform was then applied to directly detect *St* samples spiked into LB medium. Again, a linear relationship between the percentage of positive droplets and *St* concentration (R^2 value > 0.99) was observed (Fig. 5c). Reproducibility between samples remained good, even at low concentrations (10^2 cfu/mL). In fact, the data obtained from the DropCRISPR platform with both purified *St* DNA (Fig. 5b) and non-purified *St* in LB media (Fig. 5c) was comparable. These results demonstrate the capacity of the DropCRISPR platform to overcome high background fluorescence caused by complex sample media.

Based on such promising results in LB media, we decided to evaluate the performance of DropCRISPR in spiked milk. As *St* is known to grow in raw milk, we felt this particular matrix was an appropriate test model. Two different types of milk, lactose-free semi-skimmed milk (milk-1) and 0.1% skimmed milk (milk-2), were used in subsequent experiments. Milk was mixed in a 1:9 (sample:milk) ratio with known concentrations of *St* to obtain spiked milk samples (10^2–10^5 cfu/mL) (Fig. 5d). DropCRISPR displayed linear relationships across the entire concentration range in both milk matrices (R^2 value > 0.97 in both). It is notable that the fit is slightly worse than for samples in buffer and LB media. This can be attributed primarily to the detection sensitivity at the lowest sample concentration (10^2 cfu/mL), where the number of positive droplets was lower than expected. This is most likely caused by matrix effects interfering with the reactions, the consequences of which are more pronounced at low target concentrations. At higher target concentrations the targets could be accurately detected. These data further demonstrate the capacity of the DropCRISPR for absolute target quantification of *St* strains in raw biological samples.

4. Conclusions

In this work, we have developed a droplet-based digital diagnostic platform based on the combination of LAMP and CRISPR/Cas12a. This was made possible by employing a novel two-step microfluidic architecture, comprising a droplet generator for digital LAMP and a picoinjector to introduce the necessary CRISPR/Cas12a reagents. This method can avoid the problems of temperature incompatibilities and mutual interference between amplification reaction and CRISPR detection. The DropCRISPR platform is capable of accurately and reproducibly quantifying nucleic acid targets, proving that ultrasensitive detection of targets (at fM level) can be realized. A high tolerance to inhibitors was also displayed by DropCRISPR which was able to directly detect *St* strains from culture medium and spiked milk samples without additional nucleic acid extraction. To the best of our knowledge, DropCRISPR is the first microfluidic LAMP-Cas12a-based droplet digital detection platform. We believe that DropCRISPR will become a promising tool for ultrasensitive quantitative detection of nucleic acid.

CRediT authorship contribution statement

Hui Wu: Conceptualization, Methodology, Investigation, Writing – original draft. **Xiaobao Cao:** Methodology, Investigation. **Yingchao Meng:** Investigation. **Daniel Richards:** Writing – original draft. **Jian Wu:** Conceptualization, Writing – review & editing, Funding acquisition. **Zhangying Ye:** Methodology, Writing – review & editing. **Andrew J. deMello:** Resources, Writing – review & editing, Supervision.

Declaration of competing interest

The authors declare that they have no known competing financial interests or personal relationships that could have appeared to influence the work reported in this paper.

Acknowledgements

H. Wu and X. Cao contributed equally to this work. The authors thank Prof. Wolf-Dietrich Hardt (ETH Zurich) for providing us cultured *Salmonella typhimurium* strain. This work was supported by the Key R&D Program of Zhejiang Province (2021C02024, 2021C02059), the Expert Workstation of Yunnan Province (202105AF150060), and the National Natural Science Foundation of China (31571918). H. Wu also thanks the joint-Ph.D. program supported by the China Scholarship Council (202006320194).

Supporting Information

Additional information as noted in text. This material is available free of charge.

Appendix A. Supplementary data

Supplementary data to this article can be found online at https://doi.org/10.1016/j.bios.2022.114377.

References

Abate, A.R., Hung, T., Mary, P., Agresti, J.J., Weitz, D.A., 2010. Proc. Natl. Acad. Sci. U. S. A 107, 19163–19166.
Bhat, S., Herrmann, J., Armishaw, P., Corbisier, P., Emslie, K.R., 2009. Anal. Bioanal. Chem. 394, 457–467.
Chen, J.S., Ma, E.B., Harrington, L.B., Da Costa, M., Tian, X.R., Palefsky, J.M., Doudna, J. A., 2018. Science 360, 436–439.
Chen, Z.T., Liao, P.Y., Zhang, F.L., Jiang, M.C., Zhu, Y.S., Huang, Y.Y., 2017. Lab Chip 17, 235–240.
Dai, Y., Xu, W., Somoza, R.A., Welter, J.F., Caplan, A.I., Liu, C.C., 2020. Angew. Chem. Int. Ed. 59, 20545–20551.
Deng, H.M., Gao, Z.Q., 2015. Anal. Chim. Acta 853, 30–45.
Esbin, M.N., Whitney, O.N., Chong, S.S., Maurer, A., Darzacq, X., Tjian, R., 2020. RNA 26, 771–783.
Francois, P., Tangomo, M., Hibbs, J., Bonetti, E.J., Boehme, C.C., Notomi, T., Perkins, M. D., Schrenzel, J., 2011. FEMS Immunol. Med. Microbiol. 62, 41–48.
Gootenberg, J.S., Abudayyeh, O.O., Lee, J.W., Essletzbichler, P., Dy, A.J., Joung, J., Verdine, V., Donghia, N., Daringer, N.M., Freije, C.A., Myhrvold, C., Bhattacharyya, R.P., Livny, J., Regev, A., Koonin, E.V., Hung, D.T., Sabeti, P.C., Collins, J.J., Zhang, F., 2017. Science 356, 438–442.
Hellou, M.M., Gorska, A., Mazzaferri, F., Cremonini, E., Gentilotti, E., De Nardo, P., Poran, I., Leeflang, M.M., Tacconelli, E., Paul, M., 2021. Clin. Microbiol. Infect. 27, 341–351.
Hindson, C.M., Chevillet, J.R., Briggs, H.A., Gallichotte, E.N., Ruf, I.K., Hindson, B.J., Vessella, R.L., Tewari, M., 2013. Nat. Methods 10, 1003–1005.
Huggett, J.F., Cowen, S., Foy, C.A., 2015. Clin. Chem. 61, 79–88.
Kang, T.S., 2019. Trends Food Sci. Technol. 91, 574–585.

Li, L.X., Li, S.Y., Wu, N., Wu, J.C., Wang, G., Zhao, G.P., Wang, J., 2019a. ACS Synth. Biol. 8, 2228–2237.
Li, Y., Li, S., Wang, J., Liu, G., 2019b. Trends Biotechnol. 37, 730–743.
Li, Y.M., Fan, P.H., Zhou, S.S., Zhang, L., 2017. Microb. Pathog. 107, 54–61.
Li, Z., Liu, Y., Wei, Q.Q., Liu, Y.J., Liu, W.W., Zhang, X.L., Yu, Y.D., 2016. PLoS One 11, e0153359.
Lin, X.Y., Huang, X., Urmann, K., Xie, X., Hoffmann, M.R., 2019. ACS Sens. 4, 242–249.
Lobato, I.M., O'Sullivan, C.K., 2018. TrAC Trends Anal. Chem. (Reference Ed.) 98, 19–35.
Mangal, M., Bansal, S., Sharma, S.K., Gupta, R.K., 2016. Crit. Rev. Food Sci. Nutr. 56, 1568–1584.
Nixon, G., Garson, J.A., Grant, P., Nastouli, E., Foy, C.A., Huggett, J.F., 2014. Anal. Chem. 86, 4387–4394.
Notomi, T., Okayama, H., Masubuchi, H., Yonekawa, T., Watanabe, K., Amino, N., Hase, T., 2000. Nucleic Acids Res. 28, e63.
Park, J.S., Hsieh, K., Chen, L.B., Kaushik, A., Trick, A.Y., Wang, T.H., 2021. Adv. Sci. 8, 2003564.
Qian, C., Wang, R., Wu, H., Zhang, F., Wu, J., Wang, L., 2019. Anal. Chem. 91, 11362–11366.
Quan, P.L., Sauzade, M., Brouzes, E., 2018. Sensors 18, 1271.
Rane, T.D., Chen, L.B., Zec, H.C., Wang, T.H., 2015. Lab Chip 15, 776–782.
Rolando, J.C., Jue, E., Barlow, J.T., Ismagilov, R.F., 2020. Nucleic Acids Res. 48, e42.
Rolando, J.C., Jue, E., Schoepp, N.G., Ismagilov, R.F., 2019. Anal. Chem. 91, 1034–1042.
Schuler, F., Siber, C., Hin, S., Wadle, S., Paust, N., Zengerle, R., von Stetten, F., 2016. Anal. Methods 8, 2750–2755.
Sun, B., Shen, F., McCalla, S.E., Kreutz, J.E., Karymov, M.A., Ismagilov, R.F., 2013. Anal. Chem. 85, 1540–1546.
Wu, H., Chen, X., Zhang, M., Wang, X., Chen, Y., Qian, C., Wu, J., Xu, J., 2021a. TrAC Trends Anal. Chem 135, 116150.
Wu, H., Chen, Y.J., Yang, Q.Q., Peng, C., Wang, X.F., Zhang, M.Y., Qian, S.W.J., Xu, J.F., Wu, J., 2021b. Biosens. Bioelectron. 188, 113352.
Wu, H., He, J.-s., Zhang, F., Ping, J., Wu, J., 2020a. Anal. Chim. Acta 1096, 130–137.
Wu, H., Zhang, S.Y., Chen, Y.J., Qian, C., Liu, Y., Shen, H., Wang, Z.J., Ping, J.F., Wu, J., Zhang, Y.J., Chen, H., 2020b. J. Pharm. Biomed. Anal. 190, 113489.
Wu, X.L., Tay, J.K., Goh, C.K., Chan, C., Lee, Y.H., Springs, S.L., Wang, D.Y., Loh, K.S., Lu, T.K., Yu, H., 2021c. Biomaterials 274, 120876.
Yu, F.T., Yan, L.T., Wang, N., Yang, S.Y., Wang, L.H., Tang, Y.X., Gao, G.J., Wang, S., Ma, C.J., Xie, R.M., Wang, F., Tan, C.A.R., Zhu, L.X., Guo, Y., Zhang, F.J., 2020. Clin. Infect. Dis. 71, 793–798.
Yuan, H., Tian, J., Chao, Y., Chien, Y.-S., Luo, R.-H., Guo, J.-Y., Li, S., Chou, Y.-J., Shum, H.C., Chen, C.-F., 2021. ACS Sens. 6, 2868–2874.
Zhang, S.Y., Su, X.S., Wang, J., Chen, M.Y., Li, C.Y., Li, T.D., Ge, S.X., Xia, N.S., 2020. Crit. Rev. Anal. Chem. 52, 413–424.
Zhao, X.M., Xia, Y.N., Whitesides, G.M., 1997. J. Mater. Chem. 7, 1069–1074.
Zhao, Y.X., Chen, F., Li, Q., Wang, L.H., Fan, C.H., 2015. Chem. Rev. 115, 12491–12545.
Zhu, Q.Y., Gao, Y.B., Yu, B.W., Ren, H., Qiu, L., Han, S.H., Jin, W., Jin, Q.H., Mu, Y., 2012. Lab Chip 12, 4755–4763.